

N O T I C E

THIS DOCUMENT HAS BEEN REPRODUCED FROM
MICROFICHE. ALTHOUGH IT IS RECOGNIZED THAT
CERTAIN PORTIONS ARE ILLEGIBLE, IT IS BEING RELEASED
IN THE INTEREST OF MAKING AVAILABLE AS MUCH
INFORMATION AS POSSIBLE



FINAL REPORT NASA CONTRACT NGR 05-002-284

**(NASA-CR-165112) FABRICATION OF X-RAY
TELESOPES FOR SOUNDING ROCKET FLIGHTS**

N82-17002

Final Report. (California Inst. of Tech.)

21 p HC A02/MF A01

CSCL 03A

Unclass

G3/89 27279

1.0 Introduction

This contract has supported the development and fabrication of two X-ray telescopes and two detector systems as well as two sounding rocket flights of one of the telescopes (15" diameter, Wolter type I telescope). The telescopes were fabricated using the diamond point technique at Oak Ridge National Laboratory which provided the accurate figure of the mirrors to about a focal plane blur of 0.5 arc minutes.

2.0 X-ray Telescopes

The 15" telescope mirrors were polished at Cal Tech using standard polishing techniques to remove tooling marks from the diamond turning, then chemically polished to bring the X-ray reflectivity up to nearly the theoretical values. The optical image formed by the 15" telescope was found to produce a blur of about 40 arc seconds for a parallel beam of incoming laser light. The first flight of the telescope produced an X-ray image of Capella which indicated that the X-ray image was blurred to the extent of about 2 arc minutes. This additional image degradation may have been due to a slight error in focusing the X-ray image onto the detector.

The parameters of the 15" telescope are given in Table I and are displayed graphically in Figure 1. The collecting area including detector efficiency as a function of energy is given in Figure 2, however, the efficiency is not measured over the entire telescope area and may lie on the high side of the true area. The

measurement of Capella gives the best estimate of the overall system efficiency, since Capella appears to be a steady X-ray source with a well-measured spectrum (Cash *et al.* 1978, Holt *et al.* 1979). This measurement is in good agreement with the overall efficiency, but the statistics are poor, based on only 19 counts. The telescope has been flown twice without any damage, which speaks well for the recovery system and mirror protection design. The mirrors will continue to be flown several more times during the forthcoming year.

The largest mirror pair of 31" diameter, prepared for an Aries vehicle, has been machined at Oak Ridge and forms a good image in optical light. The surface will be coated with acrylic lacquer to cover the tooling marks left from the diamond turning process. The lacquer will then be coated with evaporated copper and chromium to provide a high X-ray reflectivity. The parameters of the Aries mirrors are given in table II.

A 60" diameter auto collimator system has been set up at Penn State (Figs. 3 and 4) for testing the large Aries mirrors. The optical beam is parallel to an accuracy of about 2 arc seconds. This system is used for testing the overall figure of the mirror pair. The X-ray tests can be performed in a large tank originally used by Prof. Rank for molecular spectroscopy. The vacuum tank is 100 feet long and three feet in diameter and should provide an adequate path to evaluate the reflectivity and scatter of the surface of the Aries mirrors.

3.0 First Flight

The detector system used for the first flight of the 15" X-ray system was a position sensitive proportional counter employing a series of 13 separate counters. The system is described in the attached publication. A blow up of the detector is shown in Figure 5.

4.0 Objectives and Detector Development - Second Flight

The chromospheres, transition region (TR), and Coronae of stars including the sun are still not well understood. Current theories make specific predictions on the temperature and ionization structure within these regions. Thus comparison with experiment now aids model making greatly in selecting the appropriate theory for the formation of these zones. Recently solar emission lines, characteristic of these high temperature regions, have been well studied. Investigations from satellites have led to the somewhat surprising result that hot outer atmospheres exist on many stars. Many are known to be far more active than the sun. Observations of these stars are difficult but potentially very rewarding since they test the models under conditions in which the gravity, surface activity, composition, and rotation vary considerably from the sun.

Capella is a nearby star which is known to have a very hot corona from X-ray observations with HEAO-1 and 2. It emits 10^{44} times the solar X-ray flux. It is also well studied in the optical from the ground, and in the ultraviolet with the International Ultraviolet Explorer (IUE). Because of its proximity and the low Interstellar medium (ISM) density along our line of sight, it may also be possible to detect Capella in the extreme ultraviolet (XUV). Line emission in the XUV (10-100 eV) is produced in the upper chromosphere and TR. The lines of singly ionized helium (He II) are very useful diagnostics of this region. Their production is very sensitive to the pressure-temperature structure of the chromo-TR as well as to the X-ray flux (1000 eV and higher) radiated down from the corona. The important lines are at 256 Å, 304 Å, 1640 Å corresponding to the $n = 3 \rightarrow 2$, $n = 2 \rightarrow 1$, and $n = 3 \rightarrow 2$ transitions. He II 1640 has been measured by the IUE.

In one model (Zirin, 1975) the primary mechanism for the production of these lines is photoionization of He II by coronal radiation shortward of 226 Å followed by recombination. More than 2/3 of the recombinations are to $n = 2$,

leading to a conversion of most of the coronal flux to 304 Å. Further, the flux of 1640 Å and 256 Å should be in the ratio of recombination and branching rates. This model also relates the flux of 304 Å to the absorption line at 10,830 Å of He I triplet state. This absorption line is formed in the coolest part of the chromosphere where the He is not ionized. Because of radiative selection rules the He I triplet state can only be formed by collisions or by photoionization followed by recombination. In the Zirin model there are not enough hot electrons in this part of the atmosphere to provide collisional excitation and the 10,830 Å feature is formed by photoionization of He I by the 304 Å flux emitted downward from the chromo TR. One then would expect the 10,830 Å absorption feature to be related in strength to the He II 304 Å emission line. By using the solar ratio for 304:10830 and extrapolating to Capella by using the ratio of 10,830 Capella/10,830 sun ($\approx \sim 50$), we would expect a 304 Å flux of 0.9-4.0 photons/cm² - s at earth allowing for the ISM absorption of 70%. The solar 10,830 Å emission has been measured with ground based infrared detection systems (Zirin, 1975).

We have developed a rocket spectrometer sensitive in the 176-400 Å bandpass to observe 304 Å and also possibly 256 Å (although it is 15 times less intense than 304 Å on the sun). If Capella has more hot electrons than the sun, 256 Å emission could be collisionally produced and stronger than on the sun. In addition to these chromosphere-TR lines, Dupree (Dupree 1980) has estimated the flux in Fe XII at 187Å from the corona to be ~ 0.5 ph/cm² - s. This line is a useful coronal diagnostic and its detection would be an added benefit of this flight.

Our program to search for XUV from Capella in the 180 - 450 Å bandpass region consisted of three main phases. First, an instrument with sensitivity to the levels of flux anticipated was constructed. The instrument was then calibrated to prevent large instrumental systematic errors possible in this

relatively unstudied wavelength region. Finally, the experiment was successfully flown and recovered from White Sands Missile Range on March 23, 1981.

5.0 Second Flight Detector Development

The main features in the instrument development were the construction of a two-dimensional focal plane detection system with reasonable sensitivity to 304 Å radiation (~3%) and the acquisition of diffraction gratings which, with the detector, give better than 30 Å resolution. A large collecting area in an imaging mirror system had been developed for the previous flight and 15" grazing incidence mirrors were reflown. They are described fully in the first flight write-up.

A schematic of the payload is shown in fig. 6. The transmission diffraction gratings are mounted on the front of the mirror cell covering the entire entrance aperture. The mirrors image the diffraction pattern on an imaging focal plane detector after passing through a thin AlC filter which defines our bandpass. The entire payload is evacuated to 10^{-4} before flight and at data taking altitude the vacuum is 10^{-6} - 10^{-7} .

The transmission gratings were developed at Lawrence Livermore National Laboratory after Buckbee Mears failed to produce them. The transmission gratings have a 6 micron period and are made of gold, 3 microns wide and 2 to 3 microns thick. They are constructed on 2 1/4" x 2 1/4" glass slides using photoresist illuminated through a 1-1 image mask to produce the desired pattern. Because of the delicacy of the 3 micron wire structure, support wires were added to preserve the integrity of the gratings during vibration. Vibration tests simulating our launch vehicle were performed at the Jet Propulsion Laboratory and caused no deformation or damage to the gratings.

To mount the gratings the glass slides are attached with wax to brass frames. The glass is then etched away in acid leaving a freestanding grating. The brass frames are then placed on the mirror cell with the gratings aligned in the same direction.

The XUV focal plane detector was a microchannel plate (MCP) coated with MgF₂ as a photo emitter. The plate has an efficiency of approximately 3% in most of the bandpass region. It was run in the chevron configuration (two cascaded plates) to improve the gain and position resolution. The input channels are aligned with the instrument's optic axis. Bias voltage was supplied by a small 2600 volt flight supply.

Much effort was spent developing a two-dimensional readout scheme for the plate. The two methods researched required a surface resistor to be placed behind the channel plate to collect the electrons. The disc was made at Caltech. A resistive ink with appropriate resistivity was placed on an insulating disc using a technique similar to silk screening. A second mask for the contacts was then laid over the disc and a silver-palladium ink was screened down. The disc was then fired in a dry air oven causing the inks to chemically adhere to the substrate. The uniformity of the resistive ink layer determines the linearity and uniformity of the position sensing. It required many attempts to make the flight disc. Four preamps spaced 90° apart on the disc pick up the pulse. In one method the rise times of the pulses received at the opposite contacts are determined. The further a pulse travels the broader it becomes and the difference in risetimes reflects the event position. The pulse processing unit tested provided sufficient position resolution. Unfortunately, the units required a large amount of power and would have been very difficult to keep within their operating temperature limits in vacuum environment.

In the method chosen for flight the charge collected at each preamp is integrated and the ratio of charge collected along two axes determines the location of the event. The electronics for this measurement required no special heatsinking and was readily powered from the flight battery packs. Four low noise charge preamps and ratio circuits were purchased from Surface Science Devices and integrated with our rocket electronics.

Before entering the channel plate the radiation passed through a bandpass (178 - ~400 Å filter consisting of 1500 Å of Al with a 300 Å carbon overcoat. The filter was provided by Luxel Corporation.

After construction and debugging was completed, a calibration of the instrument in the XUV was needed. This area of the spectrum is still relatively unstudied due in part to the difficulty of producing calibrated sources of intense radiation at these wavelengths. Furthermore, very thin films of contaminant hydrocarbons on the optical surfaces can greatly degrade an instrument's performance due to their high absorptivity in the XUV. Studies with higher energy X-rays would not be sensitive to this problem. The synchrotron of the National Bureau of Standards (NBS) produces a very intense spectrum of radiation over our bandpass. Because of the strength of the source and the length of their beamlines, the beam can also be sufficiently collimated to simulate a star.

A new beamline for this sort of calibration had just been completed in the late fall of 1980. The NRL and NASA had a large vacuum tank constructed at the end of a 17 meter beamline. The tank was large enough to accommodate our entire payload. The payload mounts on a gymbal inside the tank allowing it to be rotated on two perpendicular axes. In addition, the entire chamber translates in the horizontal and vertical. This facility allows the beam to be moved to different points on the mirror and, by varying the angle of incidence, to different points on the focal plane detector.

One difficulty with the system was meeting stringent vacuum requirements in the payload tank. The synchrotron requires a vacuum of 10^{-9} - 10^{-10} with hydrocarbon partial pressures a factor of 10 lower. Because of the outgassing of our instruments, we only achieved 3×10^{-9} in the tank. Thus, we couldn't open it directly to the beam. A compromise was worked out in which we used our XUV filter as a crude vacuum window. It was removed from its mount on our payload near the focal plane and placed in the beam line 10 meters upstream from the detector. We also had to sandblast the payload to clean it.

A mass spectrometer monitored the vacuum condition in the upper beam-line and we were continually shut down for contamination of the ring vacuum by hydrocarbons. This severely limited our running time.

The initial payload-beam alignment was done with a new laser system which was less than perfect. It took two days to find the beam. Once aligned we took 6 spectra through our diffraction gratings. Each was taken at a different point on the mirror to test uniformity over the inner and outer reflecting surfaces. The payload was also rotated 90° to look for differences between the two polarization states.

Figure 7 shows the raw count spectrum of one side of a typical diffraction pattern produced at the NBS. Apparent are the bandpass filter edge at 176 \AA as well as the presence of second order at 350 \AA . Figure 8 shows the synchrotron flux which produced this spectrum. By combining both sides of the pattern and taking the ratio of counts to flux the payload is calibrated without performing any individual measurements of the mirrors, XUV filter, gratings or detector. Using the new channel plate (see below), our effective area at 304 \AA was 0.05 cm^2 . For 250 seconds of signal data with a flux of $0.9\text{--}4.0 \text{ photons/sec} \cdot \text{cm}^2$ this gives an anticipated level of $11 \rightarrow 50$ counts with virtually no background in first order and even higher sensitivity in the bandpass if the zero order is used.

While at NBS a rough online data analysis showed the measured efficiency to be about 15 times lower than anticipated. Possible explanations for this were: hydrogen contamination on the optical surfaces, gain loss in the MCP, or degradation of the MgFL coating of the MCP input plate. We had noticed that $\sim 1/4$ of the channel plate seemed inefficient during data taking. To pinpoint the problem we replaced the channelplate with a tungsten photoemitter whose response had been calibrated at NBS. The current in the tungsten was consistent with the inefficiency being due to the channel plate. A new input plate was purchased from Galleleo and calibrated at the University of California relative to the old one. It had much lower internal background and was a factor of ~ 6 more efficient. The new plate was used in flight.

6.0 Preliminary Results of the Second Flight

Launch was at 8 P.M. on March 23rd. Flight went as anticipated though the background from geocoronal emission in our bandpass was about five times higher than expected. This was most likely due to our early evening launch time which was necessary because of the rapidly decreasing height of Capella at the end of our launch window.

Figure 9 shows the raw Capella diffraction spectrum from 180-500 \AA summed on either side of center. While there is a nominal detection in the bandpass, the amount of line emission at 304 \AA seems well below that expected.

A more detailed analysis of the calibration and flight data will be forthcoming.

REFERENCES

Cash, W., Bowyer, S., Charles, P., Lampton, M., Garmire, G., and Riegler, G. 1978,

Ap. J. (Letters), **223**, L21.

Holt, S. S., White, N. E., Becker, R. H., Boldt, E. A., Mushotzky, R. F., Serlemitsos,

P. J., and Smith, B. W. 1979, *Ap. J. (Letters)*, **234**, L65.

Zirin, H. 1975, *Ap. J. (Letters)*, **199**, L63.

Dupree, A. K., Preprint.

TABLE 1

PARABOLOID: $y^2 = p(2w + p)$
 $= p(2(x + 2e) + p)$

HYPERBOLOID: $\left(\frac{w - e}{a}\right)^2 - \left(\frac{y}{b}\right)^2 = 1; e^2 = a^2 + b^2; w = x + 2e$

INNER PAR./HYP:

OUTER PAR./HYP:

$p = 0.19318156 \text{ in.}$

$p' = 0.27962117 \text{ in.}$

$e = 20.00000000 \text{ in.}$

$e' = 20.00000000 \text{ in.}$

$a = 19.92314240 \text{ in.}$

$a' = 19.88901852 \text{ in.}$

$b = 1.75168326 \text{ in.}$

$b' = 2.10403001 \text{ in.}$

$X1 = 60.50000000 \text{ in.}$

$Y1 = 6.23432535 \text{ in.}$

$Y1' = 7.50213590 \text{ in}$

$X0 = 50.00000000 \text{ in.}$

$Y0 = 5.90000000 \text{ in.}$

$Y0' = 7.10000000 \text{ in}$

$X2 = 39.50000000 \text{ in.}$

$Y2 = 4.92937576 \text{ in.}$

$Y2' = 5.93234767 \text{ in}$

$\theta 1 = 0.0318 = 1.824^\circ$

$\theta 1' = 0.0383 = 2.19^\circ$

$\theta 2 = 0.0924 = 5.296^\circ$

$\theta 2' = 0.1112 = 6.37^\circ$

$A = 12.7 \text{ in}^2 = 82.22 \text{ cm}^2$

$A' = 18.4 \text{ in}^2 = 119.1 \text{ cm}^2$

TABLE 2
Aries Mirror Parameters

Inner parab/hyper*

$$p' = 0.603363825$$

$$e' = 45.5765896$$

$$a' = 45.27408698$$

$$b' = 5.2423821$$

$$X1 = 113.00 \text{ in} \qquad Y1' = 15.698 \text{ in}$$

$$X0 = 90.000 \qquad Y0' = 14.797$$

$$X2 = 71.71 \qquad Y2' = 12.528$$

$$\theta_0' = 2.33^\circ$$

$$A' = 560 \text{ cm}^2$$

Defining Equations

Paraboloid: $y^2 = p (2(x+2e) + p)$

Hyperboloid: $\left(\frac{x+e}{a}\right)^2 - \left(\frac{y}{b}\right)^2 = 1 \qquad e^2 = a^2 + b^2$

See Figure 16 for the definition of x and y.

Angular resolution is 30" at 0° , 40" at 0.50° , 3' at 1.0° and 5' at 1.5° from ray tracing evaluation. Note, plate scale is 1.5 arcmin/mm ($f = 90.0$ inches).

*The mirror which has been completed.

PARABOLOID: $y^2 = p(2w + p)$
 $= p(2(x + 2e) + p)$

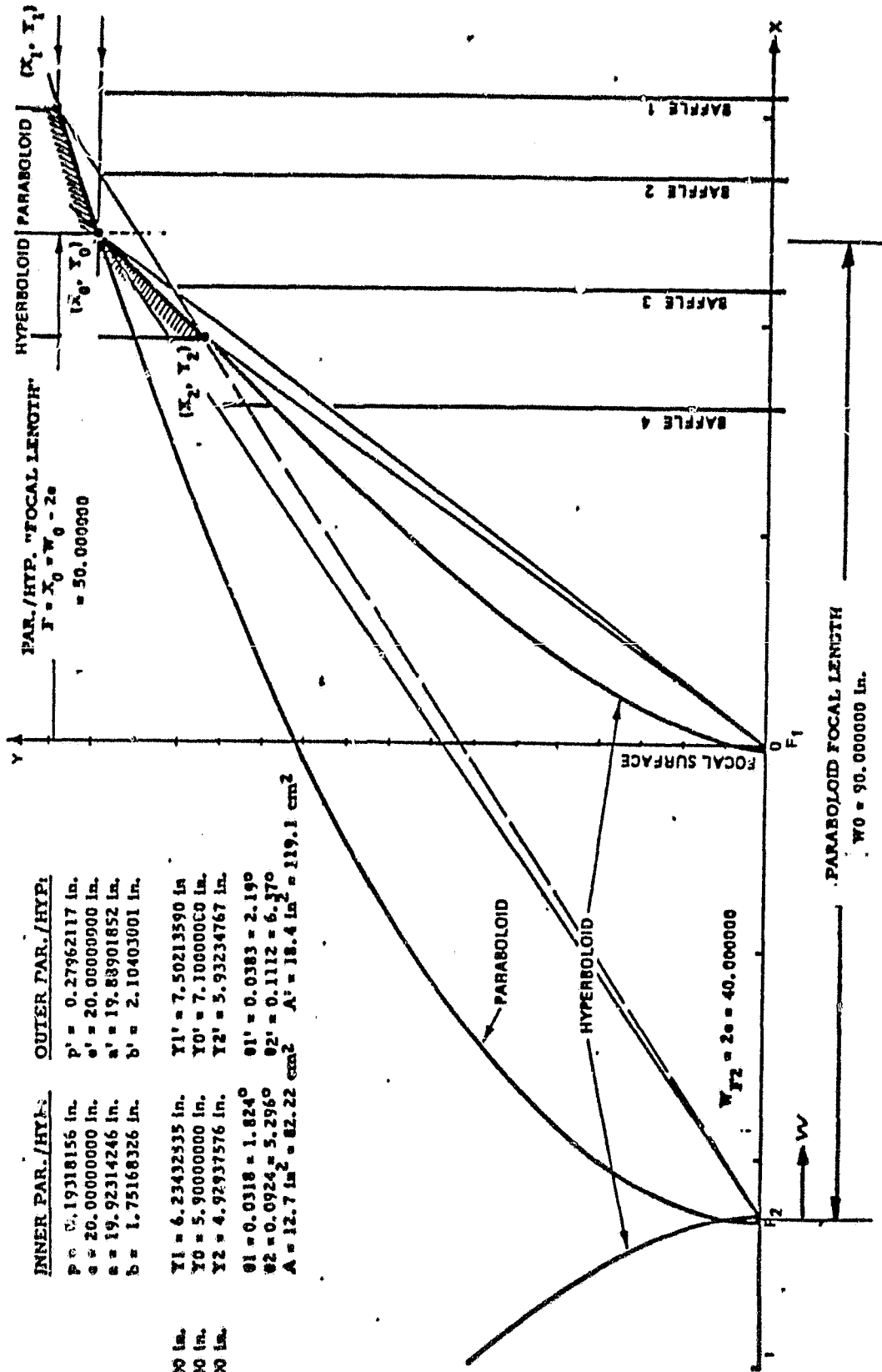
HYPERBOLOID: $\left(\frac{w-e}{a}\right)^2 - \left(\frac{y}{b}\right)^2 = 1; e^2 = a^2 + b^2; w = x + 2e$

INNER PAR./HYPER. OUTER PAR./HYP.

$p = 0.19318156$ in.
 $a = 20.00000000$ in.
 $e = 19.92314246$ in.
 $b = 1.75168326$ in.

$Y1 = 6.23432335$ in.
 $Y0 = 5.90000000$ in.
 $Y2 = 4.92937576$ in.
 $01 = 0.0318 = 1.824^\circ$
 $02 = 0.0924 = 5.296^\circ$
 $A = 12.7$ in.² = 82.22 cm² $A' = 18.4$ in.² = 119.1 cm²

$X1 = 60.50000000$ in.
 $X0 = 50.00000000$ in.
 $X2 = 39.50000000$ in.



OPTICAL DESIGN FOR THE
 ASTROBEE X-RAY TELESCOPE
 EXPERIMENT 25.001/2

Figure 1

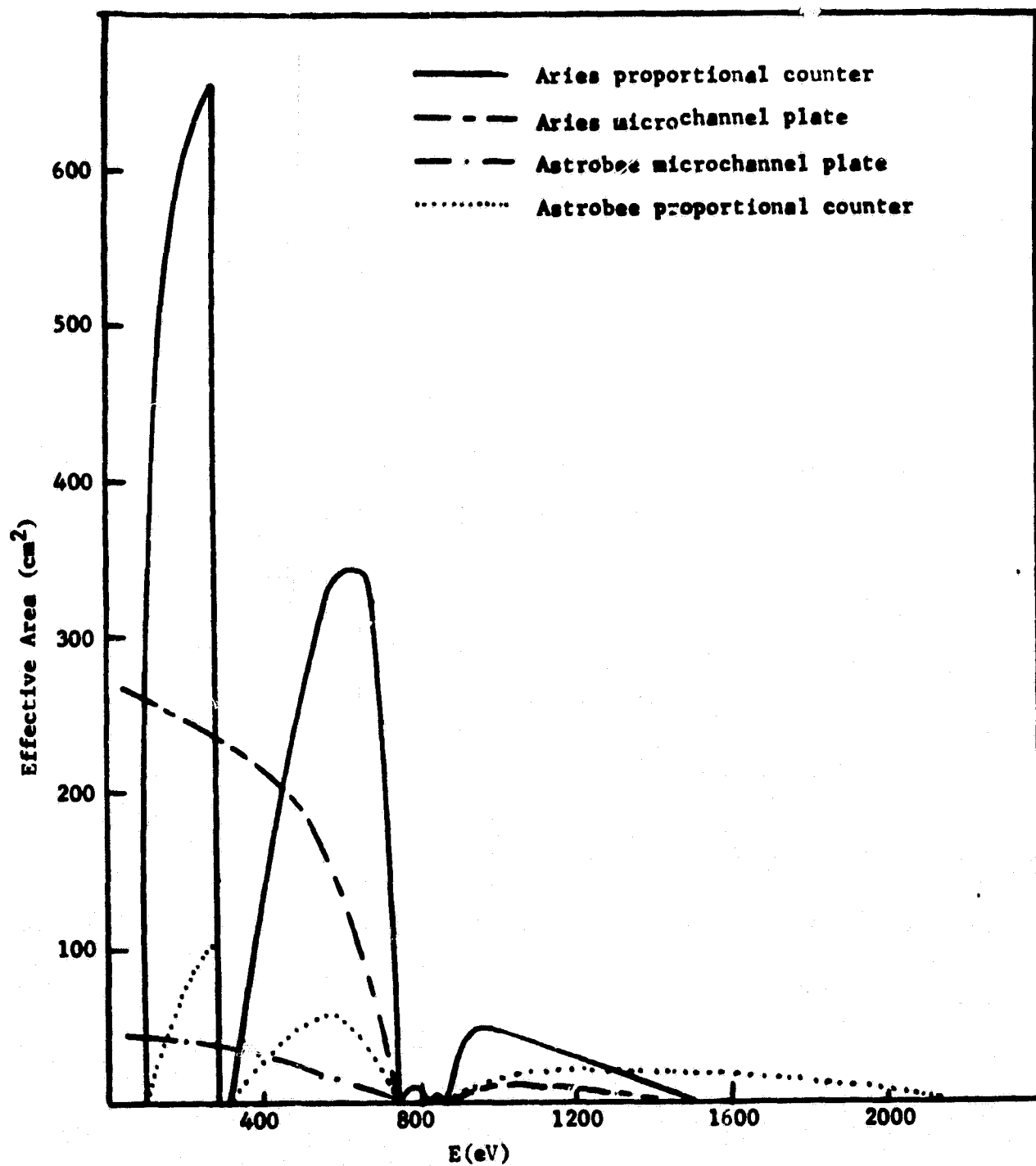


Figure 2



Figure 3

ORIGINAL PAGE
BLACK AND WHITE PHOTOGRAPH

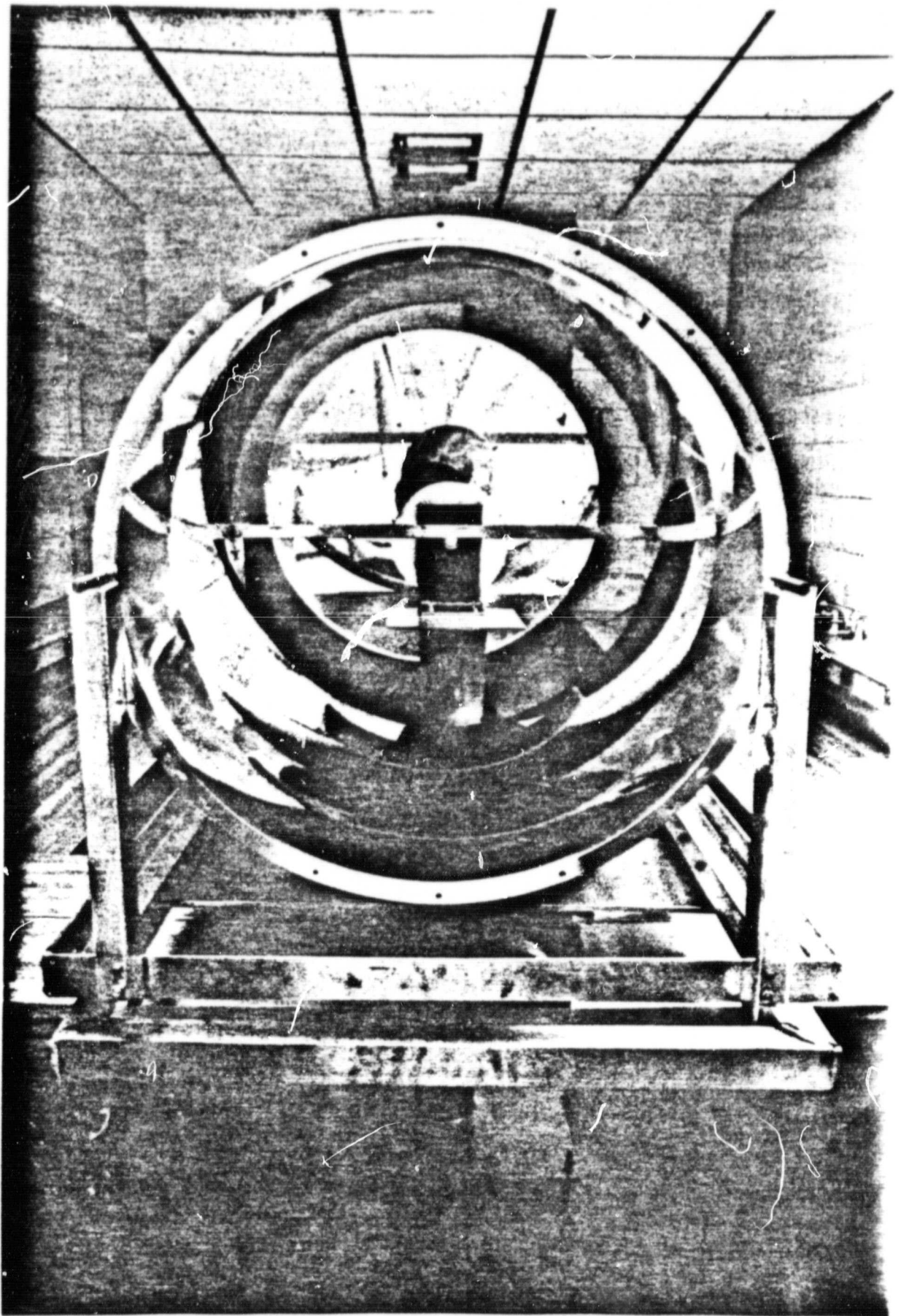


Figure 4

ORIGINAL PAGE
BLACK AND WHITE PHOTOGRAPH

ORIGINAL PAGE
BLACK AND WHITE PHOTOGRAPH

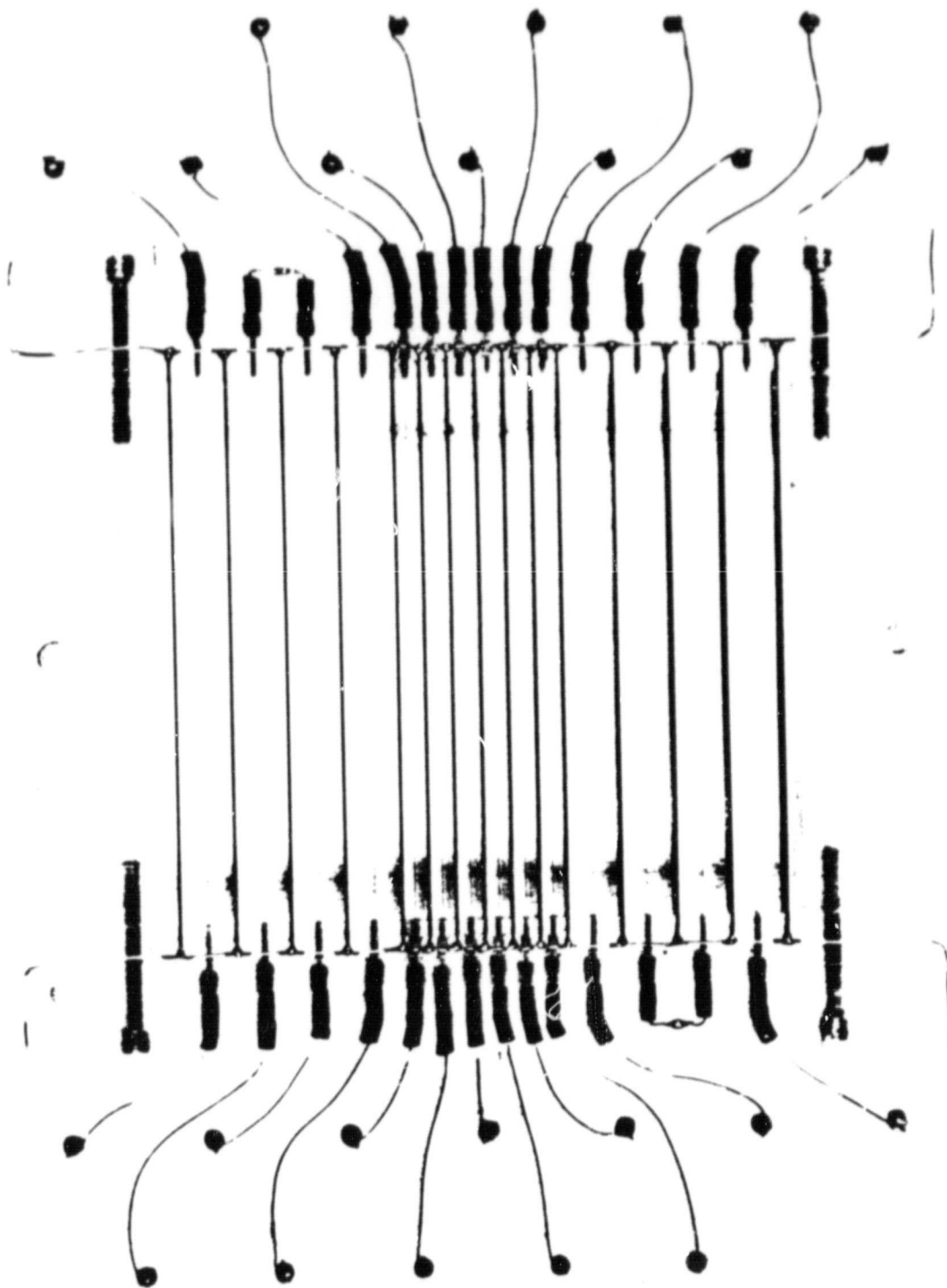
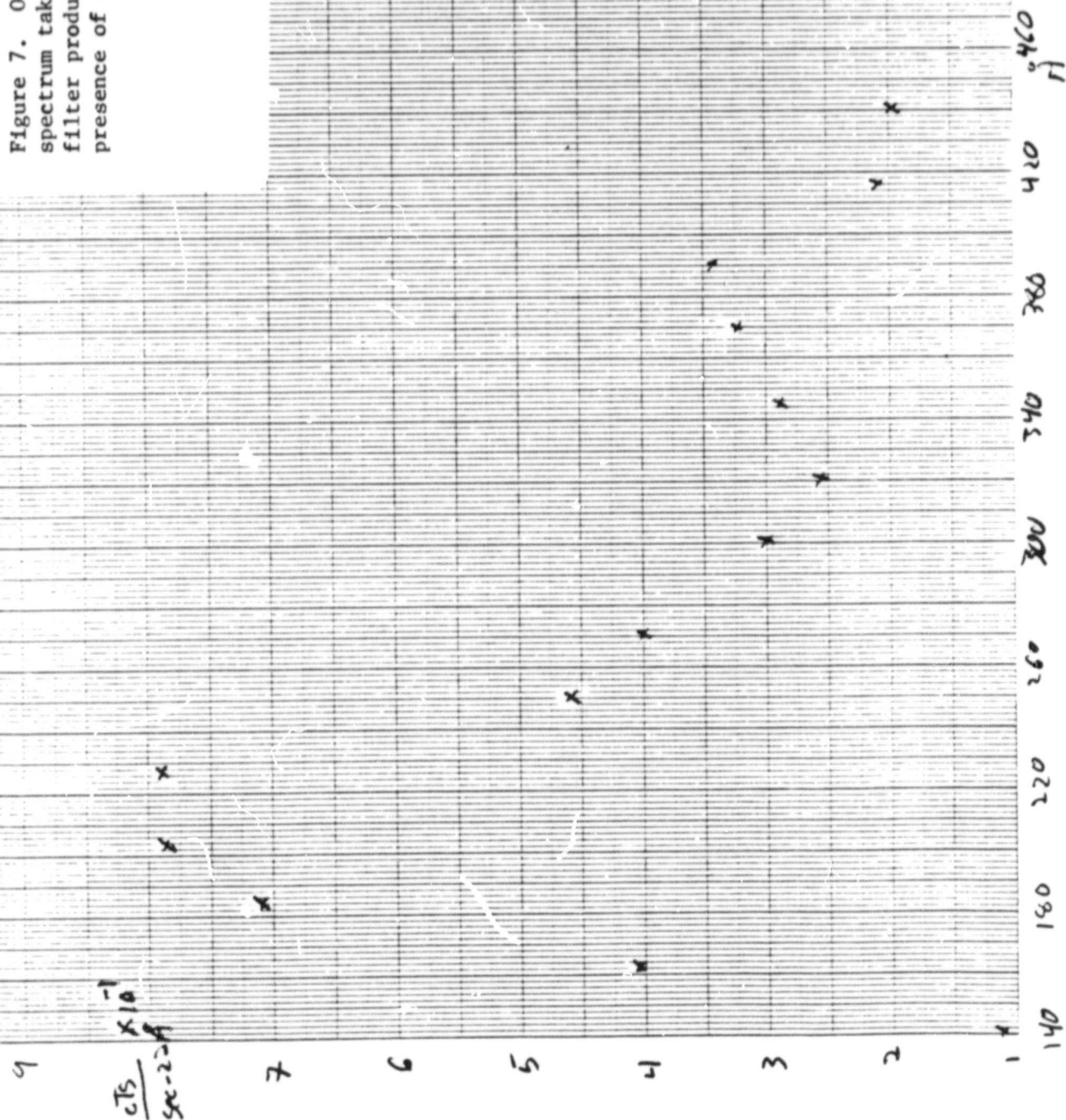


Figure 5

Figure 6. The spectrometer consists of gold diffraction gratings of six micron period followed by the X-ray mirrors from flight one. The imaged X-rays (from the mirror) pass through a bandpass defining filter and are imaged on a microchannel plate.

Figure 7. One side of a typical raw spectrum taken at NBS. Apparent are the filter produced edge at 176 Å and the presence of second order at 350 Å.

ORIGINAL PAGE IS
OF POOR QUALITY



Flux

$\frac{P_h}{\text{sec}} \times 10^{-9}$

Figure 8. The synchrotron beam flux in our bandpass.

1.6

1.4

1.2

1.0

0.8

0.6

140

140

220

260

300

340

380

420

460

A

ORIGINAL PAGE IS
OF POOR QUALITY

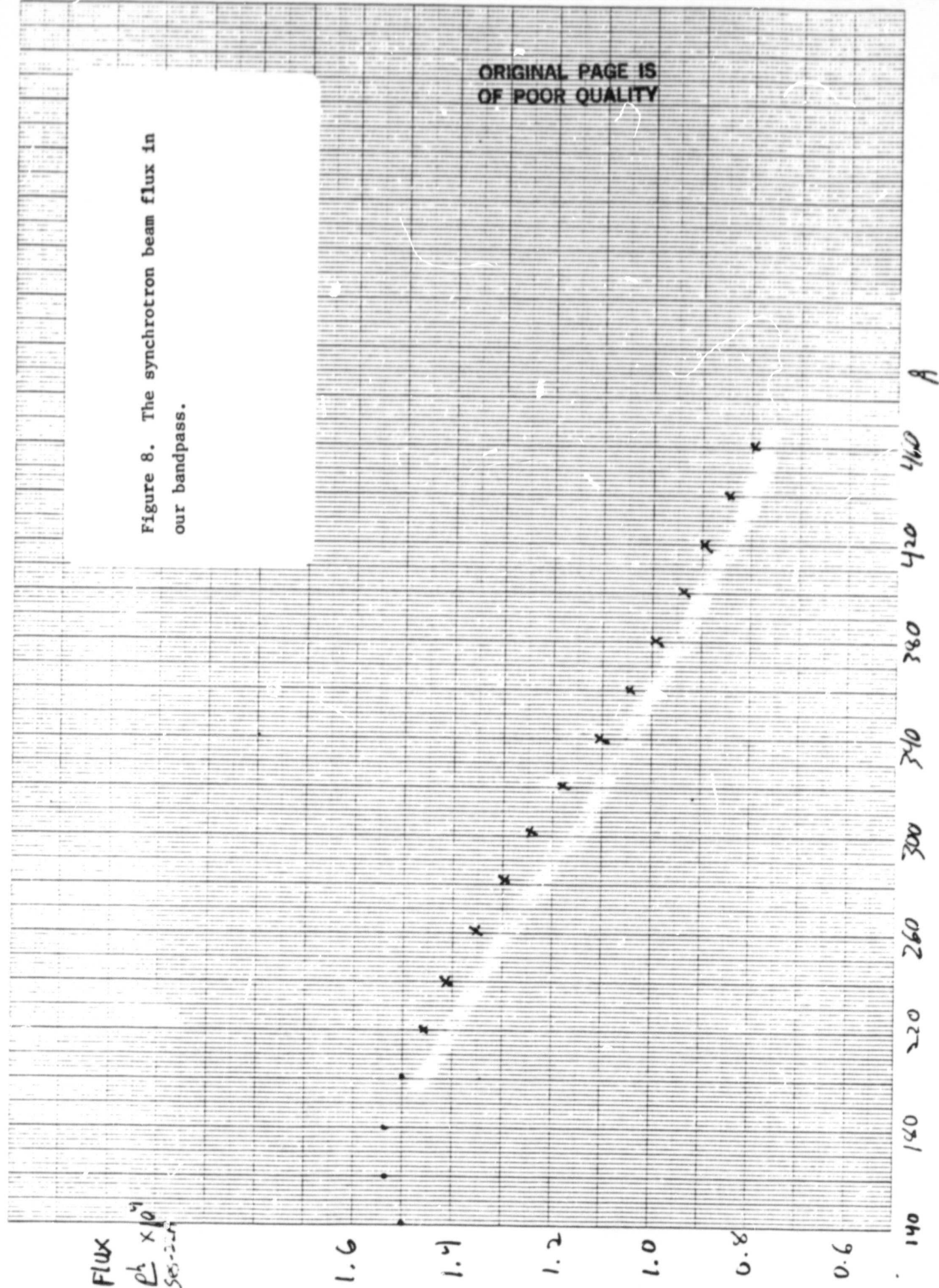


Figure 9. Raw flight count spectrum with background subtracted. Figure shows the zeroth order and the sum of both sides in first order.

ORIGINAL PAGE IS
OF POOR QUALITY

